

# Effects of Cd(II) on the stability of humic acid-coated nano-TiO<sub>2</sub> particles in aquatic environments

Li Wang<sup>1</sup> · Yixin Lu<sup>1</sup> · Chen Yang<sup>1</sup> · Chengyu Chen<sup>2</sup> · Weilin Huang<sup>1,2</sup> · Zhi Dang<sup>1</sup>

Received: 19 February 2017 / Accepted: 3 August 2017 / Published online: 21 August 2017  
© Springer-Verlag GmbH Germany 2017

**Abstract** The stability of nanoparticles (NPs) in aquatic environments is important to evaluate their adverse effects on aquatic ecosystems and human health. Nanoparticle stability is known to be influenced by coexisting ions and dissolved organic matter. This study was designed to investigate the effects of coexisting low-level Cd(II) on the stability of humic acid-coated nano-TiO<sub>2</sub> (HA-TiO<sub>2</sub>) particles in aquatic environments by measuring their aggregation kinetics through time-resolved dynamic light scattering (DLS) and monitoring suspended HA-TiO<sub>2</sub> concentrations via optical absorbance changes over time. The particles exhibited aggregation behavior consistent with the classic Derjaguin–Landau–Verwey–Overbeek (DLVO) theory. The results showed that Cd(II) concentration, pH, and ionic strength had various effects on the aggregation kinetics of the HA-TiO<sub>2</sub> NPs. The HA-TiO<sub>2</sub> particles aggregated faster as the Cd(II) concentration increased whereas the stability of the nanoparticles increased as the solution pH increased or ionic strength decreased regardless of the Cd(II) concentration. At the fixed pH and ionic strength conditions, the addition of Cd(II) promoted aggregation of nanoparticles, leading to higher attachment efficiencies. The enhanced aggregation of the HA-TiO<sub>2</sub> NPs in the presence of coexisting cadmium ions in aqueous solutions indicated that the fate and transport of nanoparticles could be greatly affected by heavy metals in aquatic environments.

**Keywords** Humic acid · Nano-TiO<sub>2</sub> · Cadmium ions · Stability · Aggregation kinetics · DLVO theory

## Introduction

Titanium dioxide nanoparticles (nano-TiO<sub>2</sub>) are widely used in many fields because of their excellent dielectric and chemical properties, such as sunscreens, pigments, coatings, disinfectants, and photocatalysts (Chen and Mao 2007, Nowack and Bucheli 2007, Tong et al. 2013, Zhu et al. 2011). The extensive application of nano-TiO<sub>2</sub> has led to their ubiquitous distribution in aquatic environments, posing adverse effects to the ecosystem. They can accumulate in aquatic organisms and might threaten human health due to their high capability of conveying toxic substances (Baun et al. 2008, Limbach et al. 2005, Liu et al. 2009). Meanwhile, Cd(II) was recognized as a common pollutant in aquatic environments that could accumulate in animal and human bodies through the food chain and cause bone diseases (Belghith et al. 2016, Lin et al. 2005, Yasukawa et al. 2005). The environmental behaviors of nanoparticles have drawn increasing attention. The fate and transport of TiO<sub>2</sub> nanoparticles in aquatic environments might be strongly dependent on their size, surface properties, and their interactions with other pollutants in aquatic environments (Battin et al. 2009, Hofmann and von der Kammer 2009).

Once released into aquatic environments, nano-TiO<sub>2</sub> particles with strong surface activity will likely interact with the ubiquitously distributed natural organic matters (NOM), such as humic acids (HA). Once organic matter adsorbs onto the surface of nanoparticles, their stability could be much different from their bare counterparts (Ferretti et al. 1997, Li et al. 2015). Previous studies have reported that HA might alter the surface properties and significantly increase the stability of nano-TiO<sub>2</sub> NPs in aquatic environments through

Responsible editor: Philippe Garrigues

✉ Chen Yang  
cyanggz@scut.edu.cn

<sup>1</sup> School of Environment and Energy, South China University of Technology, Guangzhou 510006, China

<sup>2</sup> Department of Environmental Sciences, Rutgers, The State University of New Jersey, New Brunswick, NJ 08901, USA

complexation between the acidic functional groups (mainly carboxylic acid) of HA and the hydroxyl group of nano-TiO<sub>2</sub> NPs (Hajdu et al. 2009, Hyung et al. 2007). The interaction mechanisms between HA and nano-TiO<sub>2</sub> may include anion exchange, ligand exchange, hydrophobic interaction, entropic effect, hydrogen bonding, and cation bridging (Yang et al. 2009). On the other hand, the coexisting heavy metal ions in aqueous environments might affect the stability of nanoparticles and alter their environmental risks. Cd(II) can form stable complexes with HA by strong covalent force due to the ionic polarization effect of Cd(II) having different electronic configurations (Chen et al. 2012, Jia et al. 2008, Wu et al. 2012). Several researches have demonstrated that the colloidal stability of nanoparticles in aqueous environments depends on not only the amount of NOM such as HA present mainly in surface waters but also the pH and electrolyte conditions of aqueous environments (Brigante et al. 2009, Chowdhury et al. 2013, Godinez and Darnault 2011, Keller et al. 2010, Liu et al. 2011, Zhang et al. 2009). The solution pH and electrolyte composition/concentration can modify the surface charge of nanoparticles and significantly influence their colloidal stability (Chen and Huang 2017a,b), hence directly affecting their reactivity and potential biological toxicity (Ge et al. 2011, Jiang et al. 2012).

In the present study, we investigated the effects of cadmium on the surface charge, sedimentation, and aggregation kinetics of HA-TiO<sub>2</sub> particles. Results could provide insights on the interactions among heavy metal ions, NOM, and nanoparticles in aquatic environments for predicting their potential ecological hazards.

## Materials and methods

### Materials

Nano-TiO<sub>2</sub> (anatase) and cadmium chloride were purchased from the Aladdin Reagent Company, Shanghai, China. The purity, diameter, and specific surface area of the nano-TiO<sub>2</sub> were 99.8%, 40 nm, and 97.46 m<sup>2</sup>/g, respectively. The purity of cadmium chloride was 99.9%. HA was purchased from Sigma-Aldrich (Shanghai) Trading Co., Ltd., Shanghai, China. All other solutions were prepared by analytical grade chemicals (National Medicine Corporation Ltd., Shanghai, China).

### Preparation of HA-TiO<sub>2</sub>

The HA-TiO<sub>2</sub> complexes were synthesized according to the previous publications (Li et al. 2015, Yang and Xing 2009). Briefly, the HA-TiO<sub>2</sub> was prepared by introducing 5 g of nano-TiO<sub>2</sub> into 1-L 1-g/L HA solution. It was reported that the maximum HA content on the nano-TiO<sub>2</sub> was about 50 mg/

g (Lin et al. 2012). The suspension was shaken at 150 rpm for 2 days, and then centrifuged at 4000 rpm for 30 min. The precipitated materials were then rinsed three times with Milli-Q water, freeze-dried, ground, and stored for use. The pH of supernatant was adjusted to  $1 \pm 0.5$  by addition of HCl, and then the suspension was centrifuged at 4000 rpm for 30 min. The precipitated materials were then rinsed three times with Milli-Q water, freeze-dried, and stored for use, which was named as HA<sub>treated</sub>.

### Characterization of HA and HA-TiO<sub>2</sub>

The HA and HA-TiO<sub>2</sub> were characterized using Fourier transform infrared spectroscopy (Vector 33, Bruker, Germany), and solid-state <sup>13</sup>C nuclear magnetic resonance spectroscopy (Avance AV 400, Bruker, Switzerland) was employed to investigate the functional groups.

### Zeta potential and hydrodynamic diameter measurements

The suspensions were prepared by adding 0.03-g HA-TiO<sub>2</sub> into 250 ml of different solutions: 0–100-mg/L Cd(II) in 50-mM KNO<sub>3</sub> at pH 6.90–20-mg/L Cd(II) with 50-mM KNO<sub>3</sub> solutions in different pH values, and 0–20-mg/L Cd(II) in 0–100-mM KNO<sub>3</sub> solutions at pH 6.90. The suspensions were sonicated for 1 h. The zeta potential and hydrodynamic diameter ( $D_h$ ) of HA-TiO<sub>2</sub> NPs suspension were measured using the Malvern Zetasizer Nano ZS-90 (Malvern, Westborough, MA).

### Sedimentation experiments

To evaluate the effects of pH, ionic strength, and Cd(II) concentration on the stability of HA-TiO<sub>2</sub>, sedimentation of HA-TiO<sub>2</sub> was studied by monitoring the suspended HA-TiO<sub>2</sub> concentrations via optical absorbance as a function of time (Godinez and Darnault 2011, Li et al. 2015). The suspensions were sonicated for 1 h after 0.03-g HA-TiO<sub>2</sub> was added into these background solutions. Then optical absorbance was measured at 350 nm with time intervals of 5 min over a 200-min period (Erhayem and Sohn 2014). The original absorbance of HA-TiO<sub>2</sub>,  $C_0$ , and the absorbance at different time,  $C_e$ , were used to generate the reliable calibration curves for HA-TiO<sub>2</sub> versus absorbance ( $C_0/C_e$ ), which shown the aggregation states.

### Model fitting

The DLVO model was employed for analyzing the nanoparticle stability governed by inter molecular forces between particles (Chen and Huang 2017a, b, Chen and Elimelech 2007, Liu et al. 2012, Liu et al. 2011, Shih et al. 2012, Yang-hsin et al. 2012). The classical DLVO theory involves two major

forces: the van der Waals (vdW) attraction ( $F_{vdW}$ ) and electrical double layer (EDL) repulsion ( $F_{EDL}$ ). The sum of these

two forces ( $V_{total}$ ) can determine the stability according to the following expression (Liu et al. 1995):

$$V_{total} = 4.36 \cdot 10^{-9} \psi_0^2 r \ln[1 + \exp(-kx)] - \frac{A_H}{6} \left[ \frac{2r^2}{x(x+4r)} + \frac{2r^2}{(x+2r)^2} + \ln \frac{x(x+4r)}{(x+2r)^2} \right] \quad (1)$$

where  $\psi_0$  is the zeta potential (V);  $r$  is the particle radius (m);  $k$  is the inverse of the Debye length ( $m^{-1}$ ),  $k = (2.17 \times 10^{19} I)^{1/2}$ ;  $I$  is the ionic strength ( $mol \cdot L^{-1}$ );  $x$  is the distance between two particles (m); and  $A_H$  is the Hamaker constant of particles in water (J).

### Aggregation kinetics and attachment efficiency of HA-TiO<sub>2</sub>

Time-resolved dynamic light scattering (TRDLS) was used to measure the increase in the hydrodynamic diameter ( $D_h$ ) as a function of time at 15-s time intervals in different solution chemistries. At the initial aggregation stage, the aggregation rate constant ( $k_a$ ) for HA-TiO<sub>2</sub> was proportional with time ( $t$ ) for an initial particle concentration ( $N_0$ ) (Chen and Huang 2017a, b, Chen and Elimelech 2007, Chen et al. 2006, Liu et al. 2012, Yang-hsin et al. 2012).

$$k_a \propto \frac{1}{N_0} \left( \frac{dD_h(t)}{dt} \right)_{t \rightarrow 0} \quad (2)$$

The first measurement point was considered to be at time zero ( $t = 0$ ), until the time at which  $D_h(t)$  reaches 1.25  $D_{h0}$ , where  $D_{h0}$  was 515 nm. In the few cases, especially at lower electrolyte concentrations, where aggregation was changed extremely slow, the final  $D_h$  at the end of the linear regime less than 5% of  $D_{h0}$  (Chen and Elimelech 2006). This approach was usually conducted to analyze the initial linear regime and aggregation rates.

Particle attachment efficiency ( $\alpha$ ) (i.e., inverse stability ratio,  $1/W$ ) was employed to quantify the aggregation kinetics of nanoparticles, and defined as the initial aggregation rate ( $k_a$ ) constant of interest normalized by the rate constant derived under diffusion-limited (fast) aggregation conditions ( $k_{a,fast}$ ) (Chen and Huang 2017a, b, Chen and Elimelech 2006, 2007, Liu et al. 2012, Miao et al. 2016, Yang-hsin et al. 2012).

$$\alpha = \frac{1}{W} = \frac{k_a}{k_{a,fast}} = \frac{\frac{1}{N_0} \left( \frac{dD_h(t)}{dt} \right)_{t \rightarrow 0}}{\frac{1}{N_{0,fast}} \left( \frac{dD_h(t)}{dt} \right)_{t \rightarrow 0,fast}} \quad (3)$$

Eq. (3) is simplified by dropping  $N_0$  since the initial HA-TiO<sub>2</sub> concentrations ( $N_0$ ) are maintained constant at varying ionic strengths.  $\alpha$  can be calculated from the ratio of the initial

slope of linear regime at varying ionic strengths solution to the initial slope under diffusion-limit (fast) condition.

## Results and discussion

### FTIR spectra of HA and HA-TiO<sub>2</sub>

The results of FTIR spectra for organic functional groups of HA and HA-TiO<sub>2</sub> surfaces are presented in Fig. 1. Different wave numbers had different assignment of adsorption bands (Li et al. 2004, Santos and Duarte 1998, Senesi et al. 2003). The common features of the HA and HA-TiO<sub>2</sub> included (a) the H-bonded OH stretching at 3450  $cm^{-1}$ , (b) stretching vibration of conjugated C = C or H-bonded carbonyl C = O at 1625  $cm^{-1}$ , O–H bending vibration of hydroxyl or carboxylic group, and C–O stretching of phenolic group at 1400  $cm^{-1}$ . These features indicated that HA and HA-TiO<sub>2</sub> contained hydroxyl, phenolic, and carboxyl groups.

The different features of the HA and HA-TiO<sub>2</sub> included (a) a shoulder at 2925–2850  $cm^{-1}$ , attributed to the C–H stretching of methyl or methylene groups of aliphatic chains, (b) the relative intensities of COOH stretching at 1625  $cm^{-1}$  were stronger in the HA than in the HA-TiO<sub>2</sub> spectra, (c) a weak peak in the region of 1598–1509  $cm^{-1}$  in the HA, generally attributed to aromatic C = C stretching, N–H deformation or C = N stretching of amides, but without in HA-TiO<sub>2</sub>, (d) the O–H bending vibration of alcohol or carboxylic acids, and C–O stretching vibration

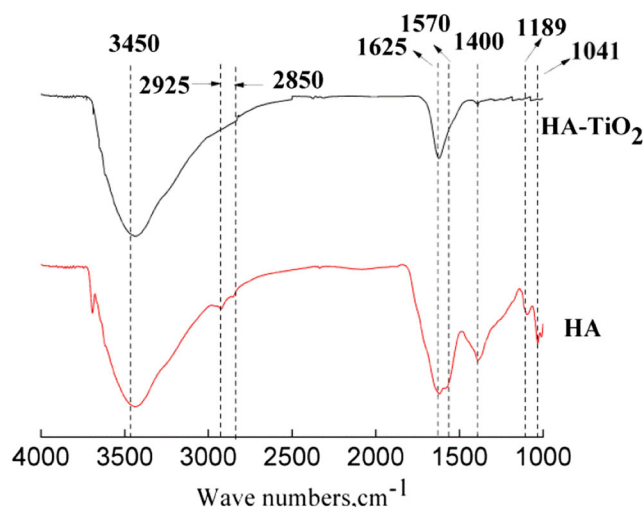


Fig. 1 FTIR spectra of HA and HA-TiO<sub>2</sub>

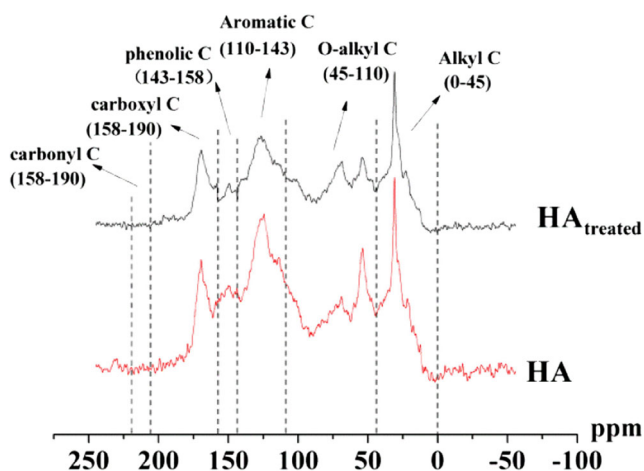


Fig. 2 Solid-state <sup>13</sup>C NMR spectra for two HAs

of phenols at 1400 cm<sup>-1</sup>, whose relative intensities were strong in the HA spectrum but very weak in the HA-TiO<sub>2</sub> spectra, and (e) the weak peak at 1189 cm<sup>-1</sup> and in the region of 1080–1030 cm<sup>-1</sup>, respectively, due to the C-OH stretching of aliphatic OH and the C-O stretching of polysaccharide-like components or to the Si-O stretching of silicate impurities, which were only present in the spectra of HA. This suggested that the interactions of COOH, aliphatic OH groups, and phenolic group on the HA with nano-TiO<sub>2</sub> were significant, which was consistent with previous studies (Kang and Xing 2008, Yang et al. 2009, Yang and Xing 2009).

### Solid-state <sup>13</sup>C NMR spectra

The solid-state <sup>13</sup>C NMR spectra are shown in Fig. 2 for two HA samples. Two HAs were obtained as original Ha and HA<sub>treated</sub>. The peaks were generally assigned to aliphatic carbon (0–45 ppm), oxygenated aliphatic carbon (45–110 ppm), aromatic carbon (110–143 ppm), phenolic C (143–158 ppm), carboxylic carbon (158–190 ppm), and carbonyl carbon (190–220 ppm). The assigned peak areas are listed in Table 1. The ratios of the aliphatic carbon, phenolic C, and carboxylic carbon of HA were larger than that of HA<sub>treated</sub>, which suggested that the COOH, aliphatic OH groups, and phenolic groups had the greatest contribution to the interaction of HA with nano-TiO<sub>2</sub>. The HA<sub>treated</sub> contained higher contents of aromatic carbon and higher aromaticity compared with HA (Table 1), which shown HA<sub>treated</sub> had higher hydrophilicity. Li (Li et al. 2004) has pointed out that the fractions with lower

molecular weight had more heterogeneous functional groups and higher contents of oxygen structure, whereas the higher molecular weight HA had lower contents of oxygen and aromatic structure. The higher molecular weight HA adsorbed by Nano-TiO<sub>2</sub> would keep the surface hydrophobic.

Aromaticity: aromatic C (110–158 ppm)/(aliphatic C (0–110 ppm) + aromatic C (110–158 ppm)).

### The influence of Cd(II) concentration on the stability of HA-TiO<sub>2</sub> nanoparticles

The effect of Cd(II) on the sedimentation of HA-TiO<sub>2</sub> particles was investigated by measuring the time evolution of their absorbance change (Fig. 3 a). The aggregation of HA-TiO<sub>2</sub> particles increased with the increasing Cd(II) concentration, which was because Cd(II) neutralized the negative surface charge of HA-TiO<sub>2</sub> particles, causing the reduced repulsive force between particles and enhanced aggregation. The zeta potentials of HA-TiO<sub>2</sub> particles are listed in Fig. 3b. Compared with nano-TiO<sub>2</sub> particles, the HA-TiO<sub>2</sub> particles had higher negative zeta potential due to deprotonation of the acidic groups (mainly carboxylic and phenolic hydroxyl) from HA, which were preferentially adsorbed on the nano-TiO<sub>2</sub> surfaces (Tombacz et al. 2000). The zeta potential of HA-TiO<sub>2</sub> particles became less negative upon the addition of Cd(II) and caused reduction in repulsive force between the particles, which could be verified by calculating the DLVO interaction energy between particles (Fig. 3c).

The results of DLVO theory fitted on the net energy between HA-TiO<sub>2</sub> particles are shown in Fig. 3c. Before the addition of Cd(II), the HA-TiO<sub>2</sub> NPs had a high EDL repulsive energy as there was a high negative zeta potential on particles. Thus, the net energy barrier prevented the sedimentation of particles. The EDL repulsive energy between particles was reduced with the addition of Cd(II), which might be due to the neutralization of negative surface charge on the HA-TiO<sub>2</sub> particles by electrostatic attraction of Cd(II) and reduction of the repulsive force between particles. Moreover, Cd(II) might bridge through to form TiO<sub>2</sub>-Cd-HA ternary complexes in the particles and then promote aggregation, which was similar with the literatures (Jia et al. 2008). Chen had reported that Cd(II) could be bonded with the acidic groups (mainly carboxylic and phenolic hydroxyl) of HA coated onto nano-TiO<sub>2</sub> through covalent bonds and form TiO<sub>2</sub>-HA-Cd complexes (Chen et al. 2012). To further investigate the effects of Cd(II) on the aggregation of the HA-TiO<sub>2</sub> particles, TRDLS was employed to gain insight into the aggregation kinetics in different

Table 1 Structural group analysis from solid-state <sup>13</sup>C NMR spectra for three HAs

Sample	Distribution of C chemical shift (ppm), %						Aromaticity
	0–45	45–110	110–143	143–158	158–190	190–220	
HA	22.73	25.48	21.60	8.87	14.43	6.89	38.1
HA <sub>treated</sub>	22.37	26.64	24.85	7.15	13.89	5.10	39.4



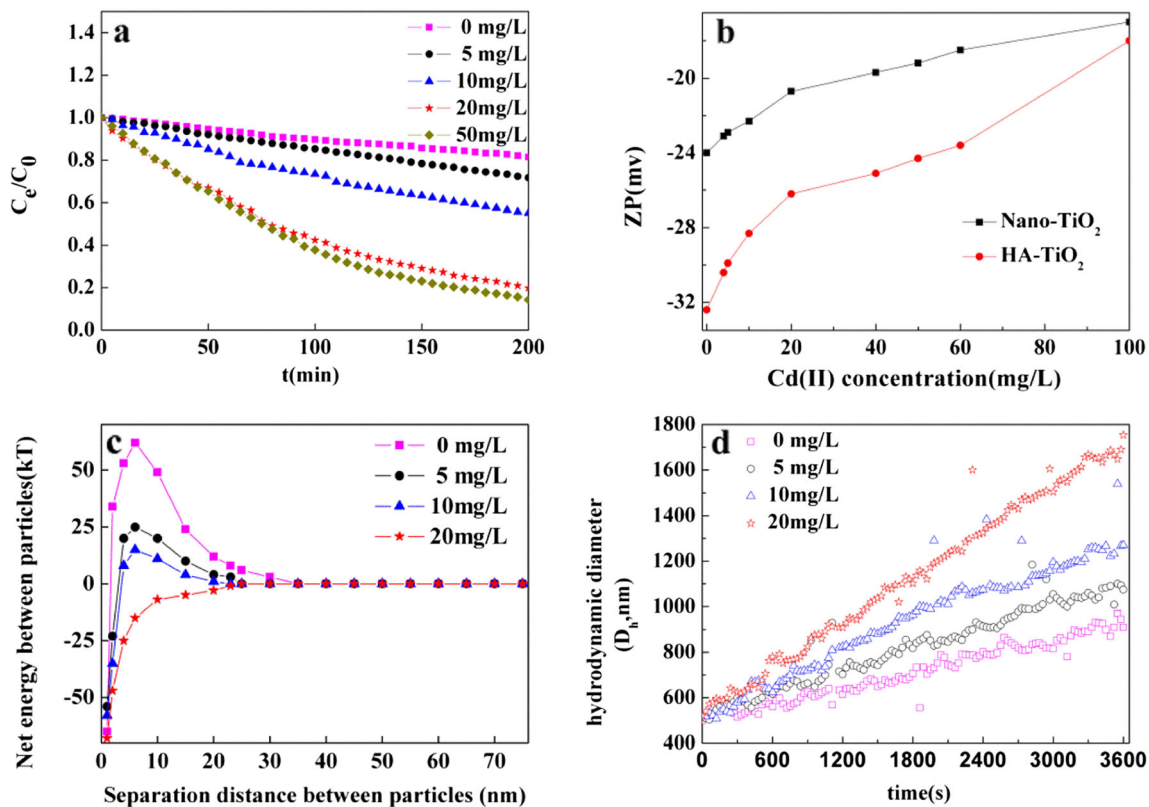


**Fig. 3** The influence of Cd(II) concentration on the stability of nanoparticles (**a** sedimentation, **b** zeta potential, **c** DLVO interaction energy between particles, and **d** aggregation profiles)

Cd(II) concentrations (Fig. 3d). The aggregation rate of the nanoparticles increased with Cd(II) concentration, which might be related with the reduction of electrostatic repulsion. This was consistent with the trend from DLVO predictions in Fig. 3c. Besides, the form of TiO<sub>2</sub>-HA-Cd or/and TiO<sub>2</sub>-Cd-HA ternary complex might also increase the aggregation kinetics of the nanoparticles (Chen et al. 2012, Jia et al. 2008, Wu et al. 2012).

### The influence of pH on the stability of HA-TiO<sub>2</sub> nanoparticles

Sedimentation studies of HA-TiO<sub>2</sub> as a function of pH are shown in Fig. 4a. The particles all gradually gathered and precipitated at three pH values. The sedimentation rate of HA-TiO<sub>2</sub> particles was the highest at pH 2, which was closed to the PZC of particles (Fig. 4b,  $pH_{PZC} = 2.9$ ) where a marked decrease in the electrostatic repulsion between particles occurred (Thio et al. 2011). The sedimentation rate of HA-TiO<sub>2</sub> particles decreased with increasing pH, which might be related to the reduced zeta potential of HA-TiO<sub>2</sub> particles (Fig. 4b). Our results were consistent with those of previous studies, which reported that the electrostatic repulsion decreased with increasing pH (Godinez and Darnault 2011). At the same pH values, Cd(II) neutralized the negative surface charge that HA imparted to nano-TiO<sub>2</sub> particles, resulting in the decrease of repulsive force and contributing to the sedimentation of HA-

TiO<sub>2</sub> particles. In addition, more acidic groups (mainly carboxylic and phenolic hydroxyl) were dissociated at higher pH, providing more complexation sites for Cd(II) so that more TiO<sub>2</sub>-HA-Cd or/and TiO<sub>2</sub>-Cd-HA ternary complexes might be formed (Chang et al. 2015, Jia et al. 2008, Wu et al. 2012), which promoted the aggregation of HA-TiO<sub>2</sub> particles.

The influence of pH on the stability of HA-TiO<sub>2</sub> was examined by measuring its zeta potentials at different pH conditions (Fig. 4b). The negative charge on the particles was screened at lower solution pH due to dissociation of more acidic groups on HA-TiO<sub>2</sub>, whereby the isoelectric point of HA-TiO<sub>2</sub> NPs was determined to be approximately pH 2.9. The acidity constants of HA were given as 4–6 for  $pK_{a1}$  (due to carboxyl groups) and 8–10 for  $pK_{a2}$  (due to phenolic groups) in the literature (Hizal and Apak 2006, Martinez et al. 2002, Ren et al. 2013, Xu et al. 2007, Zhou et al. 2005). At the same pH, the zeta potentials increased with the increasing Cd(II) concentration, which could be explained by two predominant factors. Firstly, when pH was below 2.9, the surface of the adsorbent was surrounded by H<sup>+</sup> ions such that the increase in competition between H<sup>+</sup> and Cd(II) for the limited active surface sites led to a lower adsorption percentage as the covalent bonds acted as an important role in the adsorption process. At pH beyond 2.9, the HA-TiO<sub>2</sub> surface was deprotonated so there was an electrostatic attraction between HA-TiO<sub>2</sub> and Cd(II) leading to a higher adsorption percentage (Abate and

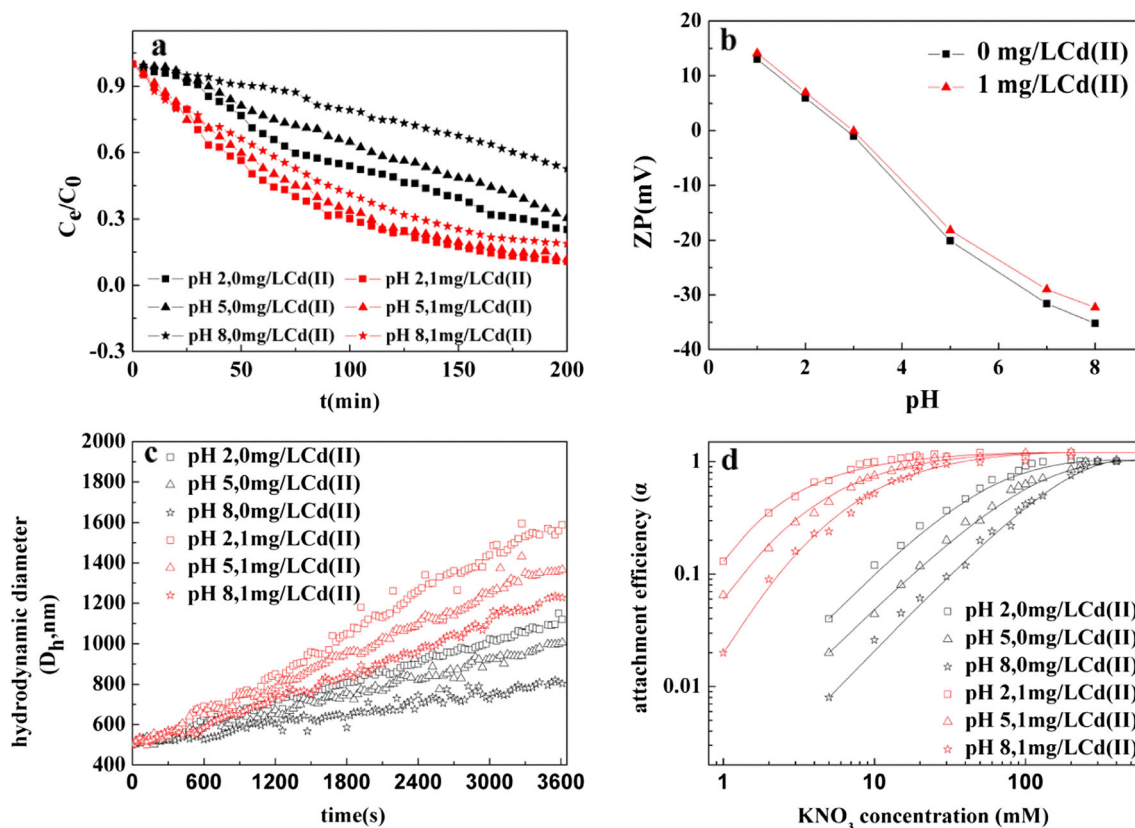


**Fig. 4** The influence of pH on the stability of nanoparticles (**a** sedimentation, **b** zeta potential, **c** aggregation profiles, and **d** attachment efficiencies)

Masini 2005, Bayazit and Inci 2014, Wang et al. 2013). Secondly, the conformations of HA coated on nano-TiO<sub>2</sub> was condensed at higher pH, which resulted in more available adsorption sites exposed for Cd(II) (Chen et al. 2012, He et al. 2016). The negative charge of HA-TiO<sub>2</sub> particles was decreased upon the addition of Cd(II), resulting in weaker repulsive force between the particles and thus faster aggregation.

In Fig. 4c, the aggregation kinetics of HA-TiO<sub>2</sub> NPs decreased with the increasing pH. At the same pH, the aggregation kinetics of HA-TiO<sub>2</sub> NPs were higher in the presence of Cd(II). The pH effects on the attachment efficiencies of HA-TiO<sub>2</sub> NPs as a function of electrolyte concentration are quantitatively shown in Fig. 4d. At pH 2, 5, and 8, the attachment efficiencies were 0.58, 0.37, and 0.22 at 50 mM KNO<sub>3</sub> concentration, respectively; the critical coagulation concentrations (CCCs) were 123.6, 158, and 263.9-mM KNO<sub>3</sub> in the absence of Cd(II). In the presence of Cd(II), however, the attachment efficiencies were all about 1 and the respective CCCs were 15.6, 19.2, and 27.4-mM KNO<sub>3</sub>. The increase in stability of HA-TiO<sub>2</sub> NPs with pH was consistent with prior reports for negatively charged particles such as fullerene NPs (Brant et al. 2005, Ma and Bouchard 2009). In addition, Cd(II) might reduce the stability of HA-TiO<sub>2</sub> NPs at the same pH by reducing the electrostatic repulsion between particles and forming TiO<sub>2</sub>-HA-Cd or/and TiO<sub>2</sub>-Cd-HA ternary complexes (Chen et al. 2012, Wu et al. 2012).

**The influence of ionic strength on the stability of HA-TiO<sub>2</sub> nanoparticles**

Different sedimentation curves for HA-TiO<sub>2</sub> particles are presented in Fig. 5a. The sedimentation rate of HA-TiO<sub>2</sub> particles increased with the KNO<sub>3</sub> concentration. In the absence of Cd(II), the concentrations of suspended particles decreased by only approximately 30% after 200 min at relatively lower ionic environment. When Cd(II) concentration was 1 mg/L, the 20-mM solution decreased the suspended particles concentration by more than 80% in 200 min. This may be explained by the changed zeta potentials of particles which affected the DLVO interaction energy between particles as discussed later in this paper (Fig. 5c).

The zeta potentials of HA-TiO<sub>2</sub> particles are presented in Fig. 5b. The zeta potential of HA-TiO<sub>2</sub> particles increased with the KNO<sub>3</sub> concentration. The EDL was compressed at higher KNO<sub>3</sub> concentration, leading to more counter ion in the EDL that neutralized the negative surface charge on particles. Thus, the repulsive force between particles was weakened and resulted in sedimentation of HA-TiO<sub>2</sub> particles (Zhang et al. 2008, Zhou and Keller 2010). In addition, the zeta potential of HA-TiO<sub>2</sub> particles increased when Cd(II) concentration increased to 1 mg/L at the same KNO<sub>3</sub> concentration. This was probably due to the electrostatic adsorption between Cd(II) and HA-TiO<sub>2</sub> (Chen et al. 2012). It was reported that the compression of the diffusive EDL and the reduction of

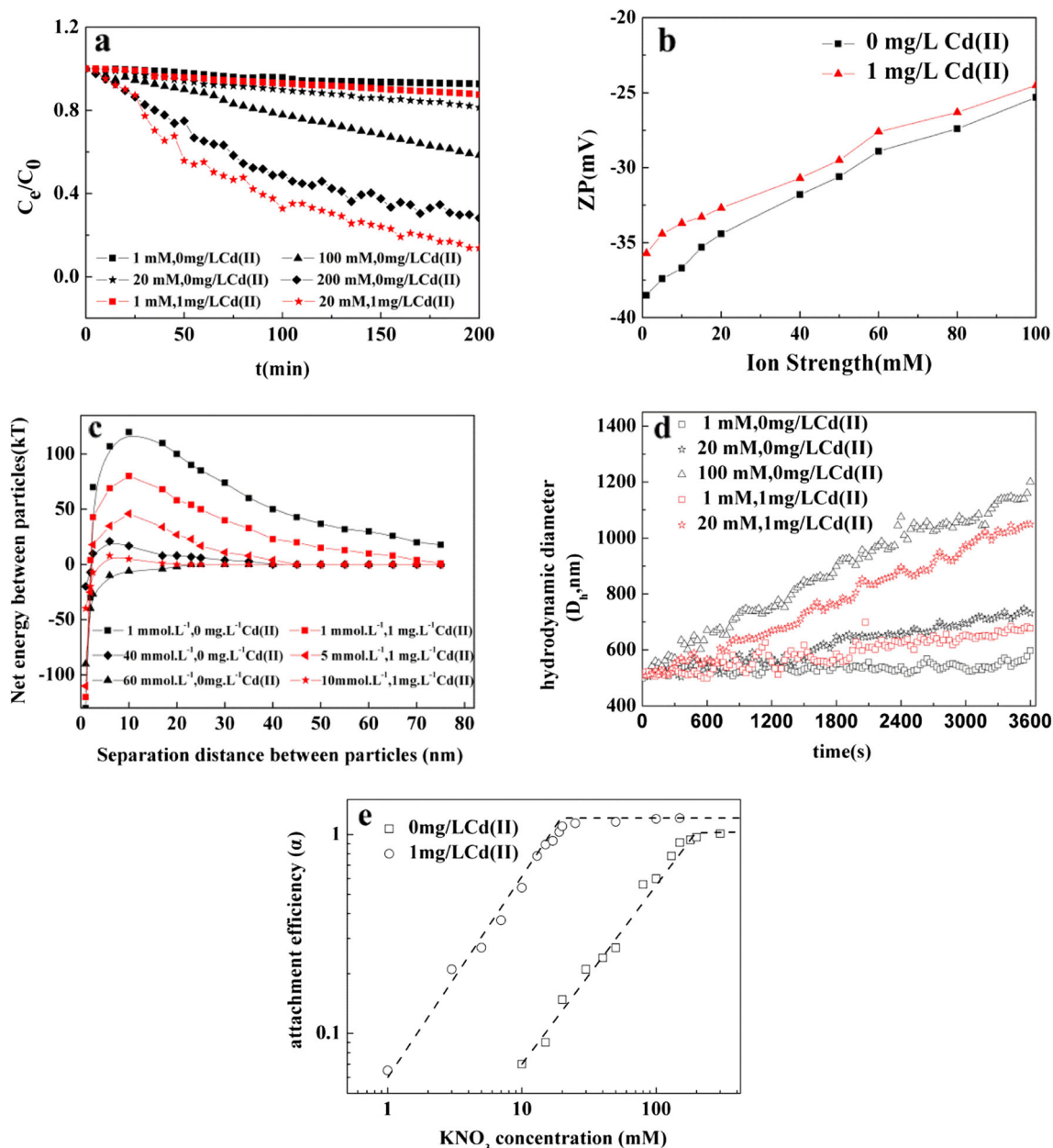


**Fig. 5** The influence of ionic strength on the stability of nanoparticles (a sedimentation, b zeta potential, c DLVO interaction energy between particles, d aggregation profiles, and e attachment efficiencies)

repulsion forces at increasing salinity would help to facilitate the formation of covalent bonds between the acidic groups on HA and Cd(II) (Filius et al. 2000). Cd(II) could increase the sedimentation rate of the nanoparticles by reducing the repulsive force between particles and forming TiO<sub>2</sub>-HA-Cd or/and TiO<sub>2</sub>-Cd-HA ternary complexes with HA-TiO<sub>2</sub> (Chen et al. 2012, Jia et al. 2008, Wu et al. 2012). Figure 5c shows the DLVO calculations for HA-TiO<sub>2</sub> particles at different KNO<sub>3</sub> concentrations. The EDL repulsive energy reduced as the KNO<sub>3</sub> concentration increased, which could promote the aggregation of particles. In the absence of Cd(II), the EDL repulsive energy was relatively small at 200 mM of KNO<sub>3</sub> and

the HA-TiO<sub>2</sub> particles were susceptible to aggregation. The addition of Cd(II) at 20 mM of KNO<sub>3</sub> completely screened the net energy barrier between the nanoparticles, leading to fast sedimentation of HA-TiO<sub>2</sub> particles. This indicated that Cd(II) could decrease the stability of nanoparticles by lowering the net energy barriers between particles.

The effect of ionic strength on the aggregation rate of HA-TiO<sub>2</sub> particles is presented in Fig. 5d. The increased KNO<sub>3</sub> concentration resulted in the faster aggregation of HA-TiO<sub>2</sub>, which could be attributed to the decreased electrostatic repulsion as was consistent with the trend from DLVO predictions in Fig. 5c (Chen and Elimelech 2006, 2009). Moreover, at higher

$\text{KNO}_3$  concentration, the increased electrolyte concentration did not further increase the aggregation rate of HA-TiO<sub>2</sub> particles because the energy barrier was completely eliminated in this diffusion-limited aggregation regime (He et al. 2008). At the same  $\text{KNO}_3$  concentration, the aggregation kinetics of HA-TiO<sub>2</sub> were higher in the presence of Cd(II), which was relevant to the weaker electrostatic repulsion due to the adsorbed Cd(II) on the HA-TiO<sub>2</sub> particles (Chen and Elimelech 2009, Chen et al. 2012). The attachment efficiencies at different  $\text{KNO}_3$  concentrations are calculated in Fig. 5e. The CCCs were 190.8 mM in the absence of Cd(II) and 19.4-mM  $\text{KNO}_3$  in the presence of Cd(II), indicating that Cd(II) could reduce the stability of HA-TiO<sub>2</sub>. As has been widely reported in other literature, the aggregation behavior of HA-TiO<sub>2</sub> was consistent with the DLVO theory (Chen and Elimelech 2007, Chen et al. 2006).

## Conclusion

In the present study, the influence of Cd(II) on the stability of HA-TiO<sub>2</sub> particles under the different environmental conditions were investigated. The aggregation behavior of HA-TiO<sub>2</sub> particles followed the classic DLVO theory, allowing for construction of predictive models for quantifying the transport of HA-TiO<sub>2</sub> NPs in an aquatic environment. The results showed that the stability of HA-TiO<sub>2</sub> NPs decreased with increasing Cd(II) concentrations, which was due to the formation of TiO<sub>2</sub>-HA-Cd or/and TiO<sub>2</sub>-Cd-HA complex with HA coated onto TiO<sub>2</sub> nanoparticles and the reduced energy barrier between the particles. In the absence of Cd(II), the stability of HA-TiO<sub>2</sub> increased with pH from 2 to 8, where the CCC increased from 58.6 to 170.9-mM  $\text{KNO}_3$ . This was possibly attributed to the deprotonation of functional groups from particle surface and the increased repulsive force between the particles. At the same pH, Cd(II) could promote the aggregation of HA-TiO<sub>2</sub> NPs, as CCCs were > 50-mM  $\text{KNO}_3$  in the presence of Cd(II) and were < 30-mM  $\text{KNO}_3$  in the absence of Cd(II). The stability of HA-TiO<sub>2</sub> NPs decreased at higher  $\text{KNO}_3$  concentrations due to compression of the EDL and lowering of the energy barrier between the particles. The Cd(II) could reduce the stability of HA-TiO<sub>2</sub> NPs even at low  $\text{KNO}_3$  concentrations, as was evidenced by the decrease in the scattered light intensity and the decreased CCC in the presence of Cd(II). The significant reduction of HA-TiO<sub>2</sub> stability by Cd(II) implied that Cd(II) could alter the environmental behavior of HA-TiO<sub>2</sub> NPs. Meanwhile, the bioavailability and toxicity of heavy metals might also be affected in real aqueous systems with both HA and nano-TiO<sub>2</sub>. Further research should focus on the bioavailability and toxicity of toxic pollutants to aqueous organisms with the coexistence of HA and NPs.

**Acknowledgements** This research was supported by the National Natural Science Foundation of China (No. 41173104) and by the

Science and Technology Planning Project of Guangdong Province, China (No. 2016B020242004).

## References

- Abate G, Masini JC (2005) Influence of pH, ionic strength and humic acid on adsorption of Cd(II) and Pb(II) onto vermiculite. *Colloids Surf A Physicochem Eng Asp* 262:33–39
- Battin TJ, Kammer FVD, Weilhartner A, Ottofueiling S, Hofmann T (2009) Nanostructured TiO<sub>2</sub>: transport behavior and effects on aquatic microbial communities under environmental conditions. *Environ Sci Technol* 43:8098–8104
- Baun A, Hartmann NB, Grieger K, Kusk KO (2008) Ecotoxicity of engineered nanoparticles to aquatic invertebrates: a brief review and recommendations for future toxicity testing. *Ecotoxicology* 17:387–395
- Bayazit SS, Inci I (2014) Adsorption of Cu (II) ions from water by carbon nanotubes oxidized with UV-light and ultrasonication. *J Mol Liq* 199:559–564
- Belghith T, Athmouni K, Bellassoued K, El Feki A, Ayadi H (2016) Physiological and biochemical response of *Dunaliella salina* to cadmium pollution. *J Appl Phycol* 28:991–999
- Brant J, Lecoanet H, Hotze M, Wiesner M (2005) Comparison of electrokinetic properties of colloidal fullerenes (n-C-60) formed using two procedures. *Environ Sci Technol* 39:6343–6351
- Brigante M, Zanini G, Avena M (2009) Effect of pH, anions and cations on the dissolution kinetics of humic acid particles. *Colloids Surf A Physicochem Eng Asp* 347:180–186
- Chang KC, Lee CL, Hsieh PC, Brimblecombe P, Kao SM (2015) pH and ionic strength effects on the binding constant between a nitrogen-containing polycyclic aromatic compound and humic acid. *Environ Sci Pollut Res Int* 22:13234–13242
- Chen KL, Elimelech M (2006) Aggregation and deposition kinetics of fullerene (C-60) nanoparticles. *Langmuir* 22:10994–11001
- Chen KL, Elimelech M (2007) Influence of humic acid on the aggregation kinetics of fullerene (C-60) nanoparticles in monovalent and divalent electrolyte solutions. *J Colloid Interface Sci* 309:126–134
- Chen KL, Elimelech M (2009) Relating colloidal stability of fullerene (C-60) nanoparticles to nanoparticle charge and electrokinetic properties. *Environ Sci Technol* 43:7270–7276
- Chen C, Huang W (2017a) Aggregation kinetics of diesel soot nanoparticles in wet environments. *Environ Sci Technol* 51:2077–2086
- Chen C, Huang W (2017b) Aggregation kinetics of nanosized activated carbons in aquatic environments. *Chem Eng J* 313:882–889
- Chen X, Mao SS (2007) Titanium dioxide nanomaterials: synthesis, properties, modifications, and applications. *Chem Rev* 107:2891–2959
- Chen KL, Mylon SE, Elimelech M (2006) Aggregation kinetics of alginate-coated hematite nanoparticles in monovalent and divalent electrolytes. *Environ Sci Technol* 40:1516–1523
- Chen Q, Yin D, Zhu S, Hu X (2012) Adsorption of cadmium(II) on humic acid coated titanium dioxide. *J Colloid Interface Sci* 367:241–248
- Chowdhury I, Walker SL, Mylon SE (2013) Aggregate morphology of nano-TiO<sub>2</sub>: role of primary particle size, solution chemistry, and organic matter. *Environ Sci Processes Impacts* 15:275–282
- Erhayem M, Sohn M (2014) Stability studies for titanium dioxide nanoparticles upon adsorption of Suwannee River humic and fulvic acids and natural organic matter. *Sci Total Environ* 468:249–257
- Ferretti R, Zhang JW, Buffle J (1997) Kinetics of hematite aggregation by polyacrylic acid: effect of polymer molecular weights. *Colloids Surf A Physicochem Eng Asp* 121:203–215
- Filius JD, Lumsdon DG, Meeussen JCL, Hiemstra T, Van Riemsdijk WH (2000) Adsorption of fulvic acid on goethite. *Geochim Cosmochim Acta* 64:51–60



- Ge Y, Schimmel JP, Holden PA (2011) Evidence for negative effects of TiO<sub>2</sub> and ZnO nanoparticles on soil bacterial communities. *Environ Sci Technol* 45:1659–1664
- Godinez IG, Darnault CJG (2011) Aggregation and transport of nano-TiO<sub>2</sub> in saturated porous media: effects of pH, surfactants and flow velocity. *Water Res* 45:839–851
- Hajdu A, Illes E, Tombacz E, Borbath I (2009) Surface charging, polyanionic coating and colloid stability of magnetite nanoparticles. *Colloids Surf A Physicochem Eng Asp* 347:104–108
- He YT, Wan J, Tokunaga T (2008) Kinetic stability of hematite nanoparticles: the effect of particle sizes. *J Nanopart Res* 10:321–332
- He E, Lu C, He J, Zhao B, Wang J, Zhang R, Ding T (2016) Binding characteristics of Cu<sup>2+</sup> to natural humic acid fractions sequentially extracted from the lake sediments. *Environ Sci Pollut Res Int* 23:22667–22677
- Hizal J, Apak R (2006) Modeling of cadmium(III) adsorption on kaolinite-based clays in the absence and presence of humic acid. *Appl Clay Sci* 32:232–244
- Hofmann T, von der Kammer F (2009) Estimating the relevance of engineered carbonaceous nanoparticle facilitated transport of hydrophobic organic contaminants in porous media. *Environ Pollut* 157:1117–1126
- Hyung H, Fortner JD, Hughes JB, Kim J-H (2007) Natural organic matter stabilizes carbon nanotubes in the aqueous phase. *Environ Sci Technol* 41:179–184
- Jia D-A, Zhou D-M, Wang Y-J, Zhu H-W, Chen J-L (2008) Adsorption and cosorption of Cu(II) and tetracycline on two soils with different characteristics. *Geoderma* 146:224–230
- Jiang X, Tong M, Kim H (2012) Influence of natural organic matter on the transport and deposition of zinc oxide nanoparticles in saturated porous media. *J Colloid Interface Sci* 386:34–43
- Kang S, Xing B (2008) Humic acid fractionation upon sequential adsorption onto goethite. *Langmuir* 24:2525–2531
- Keller AA, Wang H, Zhou D, Lenihan HS, Cherr G, Cardinale BJ, Miller R, Ji Z (2010) Stability and aggregation of metal oxide nanoparticles in natural aqueous matrices. *Environ Sci Technol* 44:1962–1967
- Li L, Zhao ZY, Huang WL, Peng P, Sheng GY, Fu JM (2004) Characterization of humic acids fractionated by ultrafiltration. *Org Geochem* 35:1025–1037
- Li Y, Yang C, Guo X, Dang Z, Li X, Zhang Q (2015) Effects of humic acids on the aggregation and sorption of nano-TiO<sub>2</sub>. *Chemosphere* 119:171–176
- Limbach LK, Li YC, Grass RN, Brunner TJ, Hintermann MA, Muller M, Gunther D, Stark WJ (2005) Oxide nanoparticle uptake in human lung fibroblasts: effects of particle size, agglomeration, and diffusion at low concentrations. *Environ Sci Technol* 39:9370–9376
- Lin AJ, Zhu YG, Tong YP, Geng CN (2005) Evaluation of genotoxicity of combined pollution by cadmium and atrazine. *Bull Environ Contam Toxicol* 74:589–596
- Lin D, Ji J, Long Z, Yang K, Wu F (2012) The influence of dissolved and surface-bound humic acid on the toxicity of TiO<sub>2</sub> nanoparticles to *Chlorella* sp. *Water Res* 46:4477–4487
- Liu D, Johnson PR, Elimelech M (1995) Colloid deposition dynamics in flow-through porous media: role of electrolyte concentration. *Environ Sci Technol* 29:2963–2973
- Liu H, Ma L, Zhao J, Liu J, Yan J, Ruan J, Hong F (2009) Biochemical toxicity of Nano-anatase TiO<sub>2</sub> particles in mice. *Biol Trace Elem Res* 129:170–180
- Liu X, Chen G, Su C (2011) Effects of material properties on sedimentation and aggregation of titanium dioxide nanoparticles of anatase and rutile in the aqueous phase. *J Colloid Interface Sci* 363:84–91
- Liu W-S, Peng Y-H, Shiung C-E, Y-h S (2012) The effect of cations on the aggregation of commercial ZnO nanoparticle suspension. *J Nanopart Res* 14
- Ma X, Bouchard D (2009) Formation of aqueous suspensions of fullerenes. *Environ Sci Technol* 43:330–336
- Martinez RE, Smith DS, Kulczycki E, Ferris FG (2002) Determination of intrinsic bacterial surface acidity constants using a Donnan shell model and a continuous pK(a) distribution method. *J Colloid Interface Sci* 253:130–139
- Miao L, Wang C, Hou J, Wang P, Ao Y, Li Y, Lv B, Yang Y, You G, Xu Y (2016) Effect of alginate on the aggregation kinetics of copper oxide nanoparticles (CuO NPs): bridging interaction and hetero-aggregation induced by Ca(2+). *Environ Sci Pollut Res Int* 23:11611–11619
- Nowack B, Bucheli TD (2007) Occurrence, behavior and effects of nanoparticles in the environment. *Environ Pollut* 150:5–22
- Ren X, Li J, Tan X, Wang X (2013) Comparative study of graphene oxide, activated carbon and carbon nanotubes as adsorbents for copper decontamination. *Dalton Trans* 42:5266–5274
- Santos EBH, Duarte AC (1998) The influence of pulp and paper mill effluents on the composition of the humic fraction of aquatic organic matter. *Water Res* 32:597–608
- Senesi N, D'Orazio V, Ricca G (2003) Humic acids in the first generation of EUROSOILS. *Geoderma* 116:325–344
- Shih Y-H, Liu W-S, Su Y-F (2012) Aggregation of stabilized TiO<sub>2</sub> nanoparticle suspensions in the presence of inorganic ions. *Environ Toxicol Chem* 31:1693–1698
- Thio BJR, Zhou D, Keller AA (2011) Influence of natural organic matter on the aggregation and deposition of titanium dioxide nanoparticles. *J Hazard Mater* 189:556–563
- Tombacz E, Dobos A, Szekeres M, Narres HD, Klumpp E, Dekany I (2000) Effect of pH and ionic strength on the interaction of humic acid with aluminium oxide. *Colloid Polym Sci* 278:337–345
- Tong T, Chu Thi Thanh B, Kelly JJ, Gaillard J-F, Gray KA (2013) Cytotoxicity of commercial nano-TiO<sub>2</sub> to *Escherichia coli* assessed by high-throughput screening: effects of environmental factors. *Water Res* 47:2352–2362
- Wang T, Liu W, Xiong L, Xu N, Ni JR (2013) Influence of pH, ionic strength and humic acid on competitive adsorption of Pb(II), Cd(II) and Cr(III) onto titanate nanotubes. *Chem Eng J* 215:366–374
- Wu D, Pan B, Wu M, Peng H, Zhang D, Xing B (2012) Coadsorption of Cu and sulfamethoxazole on hydroxylized and graphitized carbon nanotubes. *Sci Total Environ* 427–428:247–252
- Xu D, Chen C, Tan X, Hu J, Wang X (2007) Sorption of Th(IV) on Nectorite: effect of HA, ionic strength, foreign ions and temperature. *Appl Geochem* 22:2892–2906
- Yang K, Xing B (2009) Sorption of phenanthrene by humic acid-coated nanosized TiO<sub>2</sub> and ZnO. *Environ Sci Technol* 43:1845–1851
- Yang K, Lin D, Xing B (2009) Interactions of humic acid with nanosized inorganic oxides. *Langmuir* 25:3571–3576
- Yang-hsin S, Cheng-ming Z, Chih-ping T, Cheng-han L (2012) The effect of electrolytes on the aggregation kinetics of titanium dioxide nanoparticle aggregates. *J Nanopart Res* 14:924 (11 pp.)–924 (11 pp.)
- Yasukawa A, Higashijima M, Kandori K, Ishikawa T (2005) Preparation and characterization of cadmium-calcium hydroxyapatite solid solution particles. *Colloids Surf A Physicochem Eng Asp* 268:111–117
- Zhang Y, Chen Y, Westerhoff P, Hristovski K, Crittenden JC (2008) Stability of commercial metal oxide nanoparticles in water. *Water Res* 42:2204–2212
- Zhang Y, Chen Y, Westerhoff P, Crittenden J (2009) Impact of natural organic matter and divalent cations on the stability of aqueous nanoparticles. *Water Res* 43:4249–4257
- Zhou D, Keller AA (2010) Role of morphology in the aggregation kinetics of ZnO nanoparticles. *Water Res* 44:2948–2956
- Zhou P, Yan H, Gu BH (2005) Competitive complexation of metal ions with humic substances. *Chemosphere* 58:1327–1337
- Zhu X, Zhou J, Cai Z (2011) TiO<sub>2</sub> nanoparticles in the marine environment: impact on the toxicity of tributyltin to abalone (*Haliotis diversicolor supertexta*) embryos. *Environ Sci Technol* 45:3753–3758